

The structure, modelling and dynamics of 2,7-diisopropoxy-1,8-diarylnaphthalenes

2 PERKIN

Carl Thirsk,^a Geoffrey E. Hawkes,^b Romano T. Kroemer,^{b,c} Klaus R. Liedl,^d Thomas Loerting,^d Rima Nasser,^b Robin G. Pritchard,^c Melanie Steele,^a John E. Warren^e and Andrew Whiting^{*a}

^a Department of Chemistry, University of Durham, Science Laboratories, South Road, Durham, UK DH1 3LE

^b Department of Chemistry, Queen Mary, University of London, Mile End Road, London, UK E1 4NS

^c New address: Molecular Modelling & Design, Discovery Research Oncology, Pharmacia, Viale Pasteur 10, 20014 Nerviano (MI), Italy

^d Institute of General, Inorganic and Theoretical Chemistry, University of Innsbruck, Innrain 52a, A-6020 Innsbruck, Austria

^e Department of Chemistry, U.M.I.S.T., PO Box 88, Manchester, UK M60 1QD

Received (in Cambridge, UK) 4th February 2002, Accepted 12th July 2002
First published as an Advance Article on the web 30th July 2002

2,7-Diisopropoxy-1,8-dibromonaphthalene **5** was prepared in two steps from 2,7-dihydroxynaphthalene and was coupled under Suzuki cross-coupling conditions with boronic acids **9** and **10** to provide the corresponding 1,8-diarylnaphthalene systems **12a** and **13a** respectively. In contrast, attempted coupling of dibromide **5** with *o*-tolylboronic acid **11** proved unrewarding. Single crystal X-ray structure determination of compounds **12a** and **13a** showed that both structures possessed a high degree of structural deformation due to high internal steric repulsions between the 1,8-diaryl rings and their substituents. Dynamic ¹H NMR experiments showed that these two systems possessed very slow phenyl–naphthalene bond rotation (*ca.* 2 s⁻¹), corresponding to rotation barriers (ΔG^*) of 16–18 kcal mol⁻¹. Molecular modelling predicts that such systems have approximately similar rotation barriers and that in order to completely prevent phenyl–naphthalene bond rotation, an *ortho*-phenyl substituent is required, with a barrier to rotation of *ca.* 40 kcal mol⁻¹.

Introduction

Recent studies from our laboratories¹ have shown that 1,8-diphenylnaphthalenes and related 5,6-diphenylacenaphthenes substituted in the *meta*-position on the *peri*-phenyl rings will always undergo rotation. Further examination of the transition state model for this process shows that the positions which have the greatest effect on the rotation barrier if substituted are the *ortho*-positions on the *peri*-phenyl rings or the 2- and 7-positions on the naphthalene ring. Clough and Roberts² showed that having a methyl on the *ortho*-position on the *peri*-phenyl ring did increase the rotation barrier (24.1 kcal mol⁻¹), but rotation was still not completely halted. Hence, we undertook a study involving placing substituents in the 2- and 7-positions of the naphthalene ring, *i.e.* as in structure **1**, with the aim of halting atropisomer interconversion. There is no precedence for the preparation of 2,7-disubstituted-1,8-diarylnaphthalenes such as **1**, however, House *et al.*³ have synthesised analogous anthracene derivatives such as **2**. Such systems do exhibit stable *syn*- and *anti*-atropisomeric forms in solution up to 200 °C.

It was therefore envisaged that the synthesis of a series of compounds of type **1**, with substituents placed in the 2- and

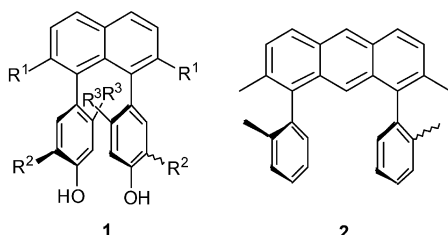
7-positions (R¹) of the naphthalene ring, and different substituents in the *ortho*-aryl (R³) positions would allow us to identify how to stabilise this class of atropisomeric system. The addition of the *meta*-aryl (R²) and phenol functions would then provide a suitably asymmetric and metal-chelating environment for asymmetric catalysis. A suitable synthetic precursor was identified as 2,7-dihydroxynaphthalene, the phenol groups of which would allow various ether derivatives to be readily prepared. In this paper we describe a detailed examination of the synthesis, structure, dynamics and modelling of such systems.

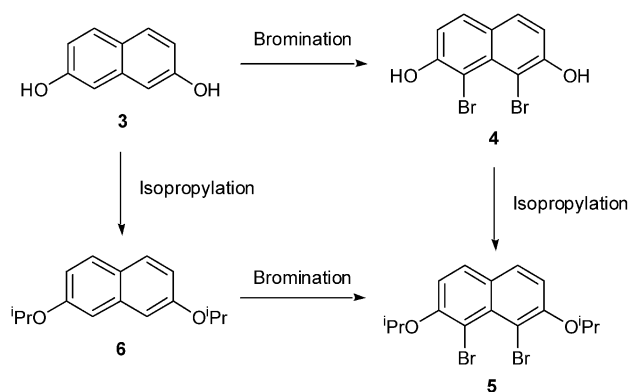
Results and discussion

Synthesis of 2,7-dialkoxy-1,8-diarylnaphthalene systems

It was therefore our intention to prepare a series of new compounds based upon general structure **1** designed to probe what actual functionality is required to prevent aryl–naphthalene bond rotation. In order to achieve the synthesis of systems of type **1**, we chose to use Suzuki methods, as previously reported in the acenaphthene series¹ and therefore required access to a 1,8-dihalonaphthalene such as **5**. It was therefore necessary to carry out a dibromination on either 2,7-dihydroxynaphthalene or a suitable diether derivative thereof, regioselectively in the 1,8-positions (Scheme 1). However, it is reported that bromination and chlorination of 2,7-dihydroxynaphthalene derivatives do not occur with the required regiocontrol.⁴

Various conditions using several brominating agents, solvents and bases were screened in order to achieve the required transformation of **3** to **4**, on ¹H NMR scale reactions. It was found that the only brominating agent to selectively brominate





Scheme 1

in the 1,8-positions was *N*-bromosuccinimide. Upon scale up and optimisation of the reaction, it was discovered that the best conditions to prepare **4** were NBS and 30 mol% pyridine in chloroform; these were in fact the only conditions which pushed the reaction to completion and produced **4** in a pure form (61%) by direct crystallisation from dichloromethane–hexane after work up (attempted silica gel chromatography produced rapid and complete decomposition of **4**).

Following successful bromination, attempts to isopropylate compound **4** (Scheme 1) under a range of conditions merely produced black insoluble precipitates from which ether **5** could not be isolated. It was however possible to acetylate **4** (pyridine–acetic anhydride) to afford the stable diacetate **7**. Single crystal X-ray structural analysis provided conclusive evidence that bromination had indeed occurred in the 1- and 8-positions (Fig. 1 and Table 1). However, dibromodiacetate **7** was

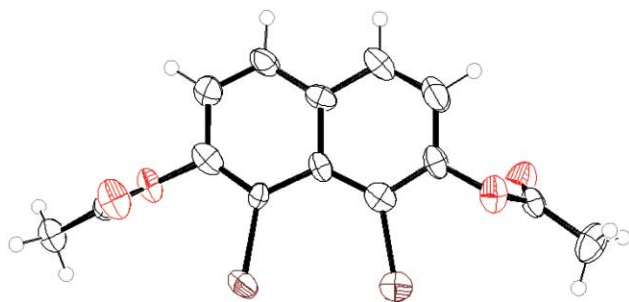
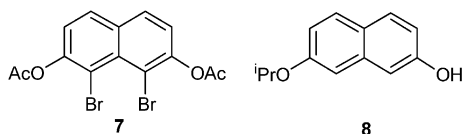


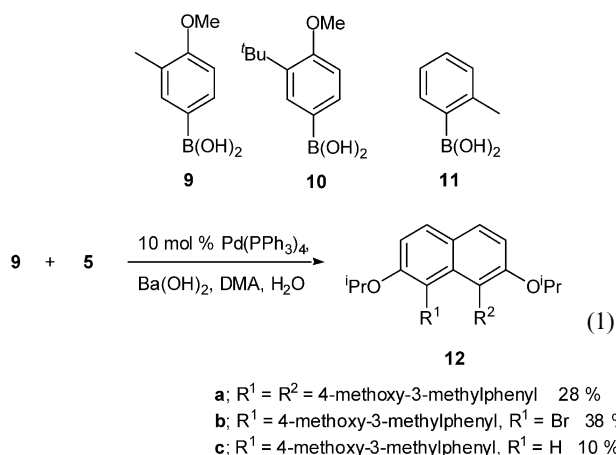
Fig. 1 X-ray crystal structure of dibromide **7**.

not considered to be a suitable candidate for cross coupling under the basic conditions used for the Suzuki reaction or for subsequent functionalisations.

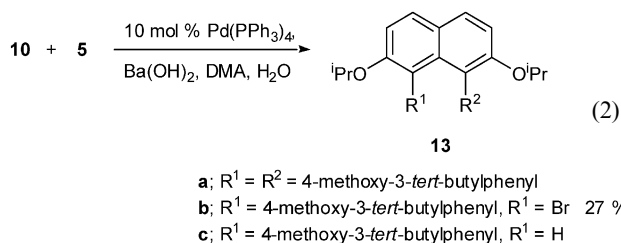


Due to the problems associated with isopropylating the dibromide **4**, an alternative approach to **5** was required. Hence, isopropylation of **3** was carried out prior to 1,8-dibromination using isopropyl bromide–potassium carbonate in DMF to yield compound **5** (61%), in addition to the mono-ether **8** (18%). Dibromination of **6** was then achieved using NBS–pyridine as before to afford **5** without any obvious sign of unwanted regioisomeric bromination products. The ¹H NMR of the crude reaction product did however show signs of some mono-brominated product remaining, which was solved by premixing the four equivalents of pyridine and NBS before the addition of diether **6**. This procedure resulted in increasing the yield of desired dibromide **5** to 40% after rapid, short column chromatography and recrystallisation.

Having prepared the dibromide **5**, attempts were made to carry out Suzuki cross couplings using the boronic acids **9–11**. Identical conditions were used to those reported previously,¹ *i.e.* 10 mol% Pd(PPh₃)₄, 2.3 equivalents of boronic acid, Ba(OH)₂, H₂O and DMA. Cross coupling of boronic acid **9** with dibromide **5** resulted in the formation of the desired compound **12a** but only in 28% yield (eqn. (1)). Other products were identified as the mono-bromo coupled compound **12b** (38% yield) and the debrominated mono-coupled compound **12c**. It should be noted that in the previous acenaphthene series,¹ the formation of mono-bromo compounds was never observed, which indicates that **12b** must be particularly sterically hindered and that formation of the 1,8-diaryl coupled product **12a** is not particularly favoured. The ¹H NMR spectrum of **12a** showed two sharp single methyl resonances at 300 MHz, which could indicate the presence of two atropisomers present in solution. However, such assumptions had proved inaccurate in the acenaphthene series of compounds,^{1a,b} thus it was necessary to prove that rotation was either not occurring, or was slow relative to the NMR timescale (*vide infra*).



The cross coupling of compounds **5** and **10** was also undertaken (eqn. (2)), in order to see if larger *tert*-butyl substituents would influence the rotation barrier in the resulting diaryl system (*i.e.* **13a** versus **12a**). The coupling reaction again produced a mixture of compounds, with purification and separation proving more difficult due to the extremely low polarity of all products. Attempts to separate the crude reaction mixture using silica gel column chromatography and pure hexane as the eluent eventually resulted in the isolation of mono-coupled product **13b** (27% yield). However, two further compounds, thought to be the desired compound **13a** and de-brominated product **13c**, could only be isolated as an inseparable mixture. Separation of **13a** and **13c** was achieved using preparative reverse phase HPLC (methanol eluent), resulting in isolation of the desired pure compounds **13a** and **13c**, unfortunately only on sufficient scale to carry out dynamic NMR studies (*vide infra*).



Finally, attempts were made to couple dibromide **5** with commercially available *o*-tolylboronic acid **11** under identical reaction conditions to those used for the synthesis of **12a** and **13a**. Unfortunately, after several attempts and over extended

Table 1 Selected crystallographic data for **7**, **12a** and **13a**

	Dibromide 7	<i>anti</i> - 12a	<i>anti</i> - 13a
Temperature/K	293	293	203(2)
Crystal size/mm ³	0.4 × 0.3 × 0.2	0.4 × 0.25 × 0.25	0.4 × 0.20 × 0.05
Molecular formula	C ₁₄ H ₁₀ Br ₂ O ₄	C ₃₂ H ₃₆ O ₄	C ₃₈ H ₄₈ O ₄
<i>F</i> _w	402.04	484.61	568.76
Crystal system	Monoclinic	Monoclinic	Orthorhombic
Space group	<i>C2/c</i>	<i>C2/c</i>	<i>Pna2</i> ₁
<i>a</i> /Å	21.383(3)	22.097(2)	16.808(2)
<i>b</i> /Å	5.411(2)	11.505(2)	22.023(2)
<i>c</i> /Å	23.737(2)	34.188(2)	9.000(3)
β /°	96.90	102.19	90
<i>Z</i>	8	12	4
λ /Å	1.959	1.54178	0.71073
μ /m ⁻¹	5.955	0.581	0.072
Reflections collected	2460	10030	6087
Independent reflections	2391	6674	3107
Reflections observed ^a	1332	2842	1972
θ range for data collection/°	2–25	3–65	1.5–25
Restraints (parameters)	(0) 183	(0) 501	(1) 515
<i>R</i> ₁ (observed reflections)	0.074	0.082	0.049
<i>wR</i> ₂ (all reflections) ^b	0.195	0.264	0.101
Goodness-of-fit on <i>F</i> ²	0.959	1.269	1.009

^a $I > 2\sigma(I)$. ^b $wR_2 = \{\sum[w(F_o^2 - F_c^2)^2]/\sum[w(F_o^2)^2]\}^{1/2}$.

reaction times no reaction was observed, as was also the case when alternative bases (BaCO₃ and Ag₂CO₃) were used. The lack of reactivity encountered in this case is paralleled by many other reports of the difficulty of achieving Suzuki coupling on such hindered systems.⁵ However, having obtained compounds **12a** and **13a**, dynamic NMR studies were undertaken and compared with single crystal X-ray analysis and molecular modelling to give an insight into the energies and likely transition states involved in the rotation process in these types of systems.

Crystal structure analysis†

Compound **12a** was slowly recrystallised from diethyl ether–methanol to give suitable crystals for X-ray analysis. Similarly, crystals of **13a** were grown by slow evaporation from methanol. The crystallographic data for compounds **12a** and **13a** are presented in Table 1. The asymmetric unit for compound **12a** is shown in Fig. 2, where it can be seen that there are two con-

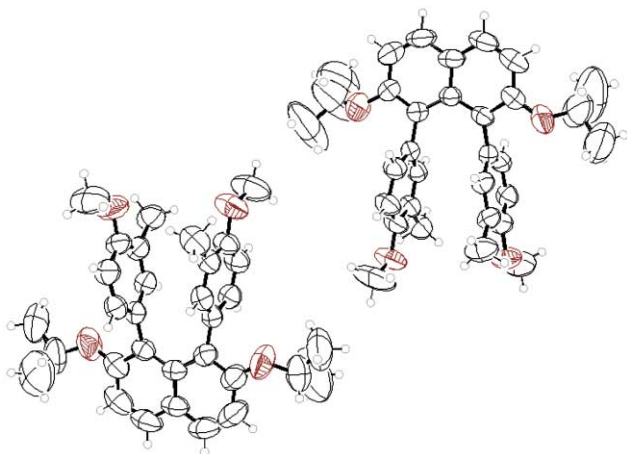


Fig. 2 Asymmetric unit of crystal structure of compound **12a** showing two conformations.

formations present, both of which have the *anti*-configuration [(conformation 1) and (conformation 2), see Figs. 3 and 4 respectively]. Similarly, compound **13a** was also obtained with

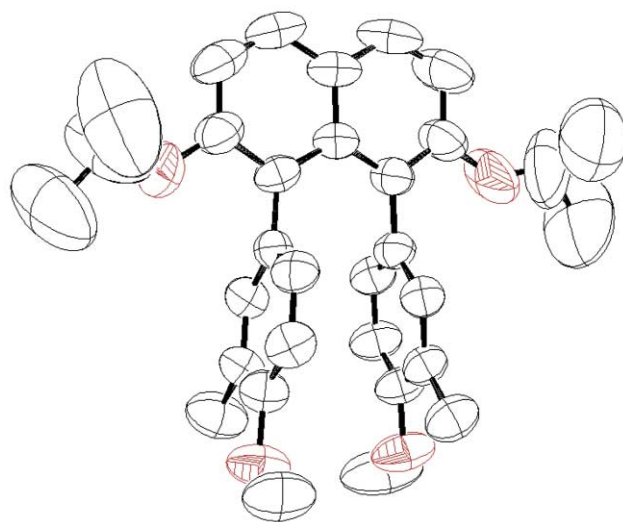


Fig. 3 Crystal structure of **12a** (conformation 1).

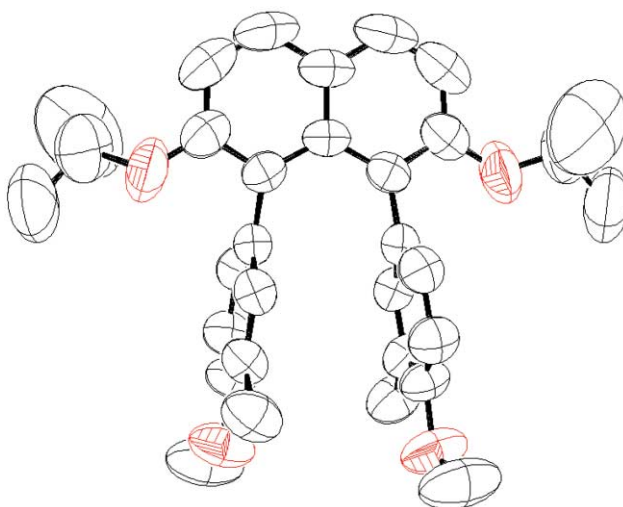


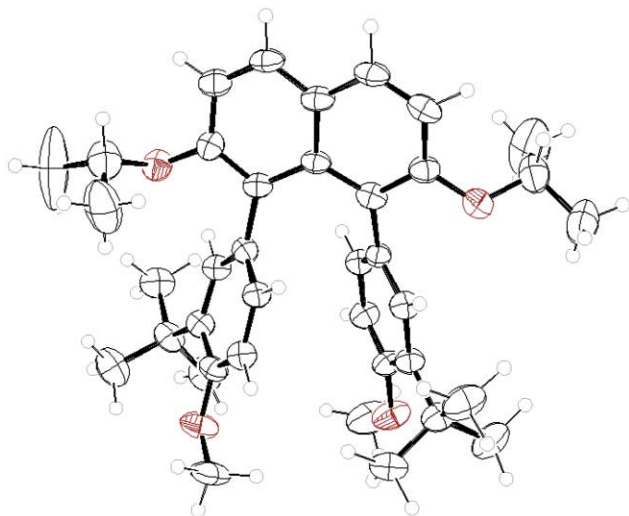
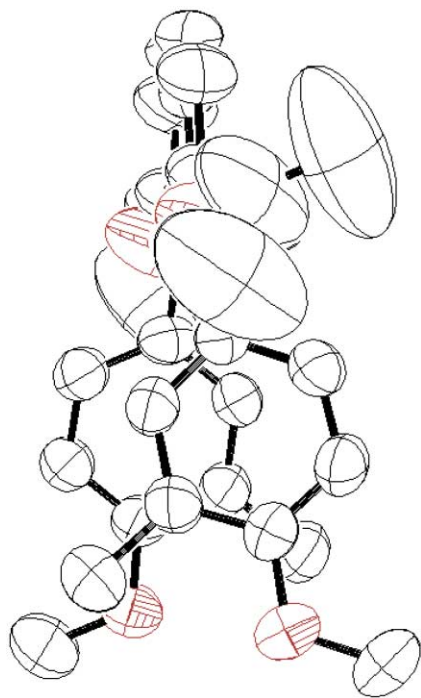
Fig. 4 Crystal structure of **12a** (conformation 2).

† CCDC reference numbers 178815–178817. See <http://www.rsc.org/suppdata/p2/b2/b201235a/> for crystallographic files in .cif or other electronic format.

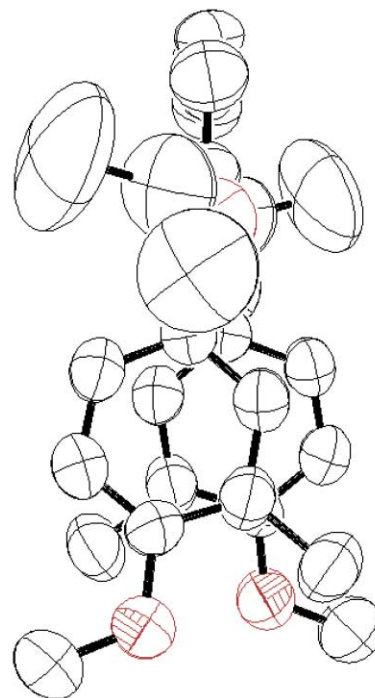
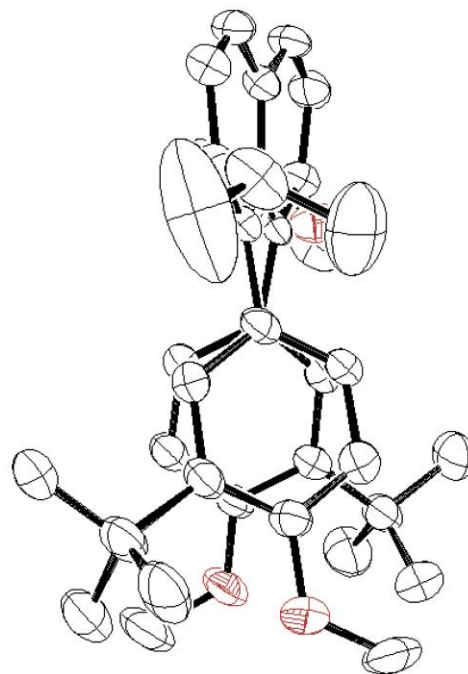
anti-geometry, as shown in Fig. 5. Figs. 6, 7 and 8 also show crystal structures of **12a** and **13a**, viewed along the naphthalene ring plane. From these X-ray data, it is clear that both mol-

Table 2 Selected geometrical parameters for **12a** and **13a**

	$\theta/^\circ$	$\phi/^\circ$	$\tau_1/^\circ$	$X/\text{\AA}$	O–O/ \AA
<i>anti</i> - 12a (conformation 1)	13.50	9.11	84.7	2.933	4.421
<i>anti</i> - 12a (conformation 2)	15.32	9.46 ^a	84.7 ^a	2.959	4.392
<i>anti</i> - 13a	12.93	7.92 9.42	52.1 53.7	2.985	4.032

**Fig. 5** Crystal structure of **13a** looking onto the naphthalene plane.**Fig. 6** Side view of **12a** (conformation 1).

ecules **12a** and **13a** relieve the steric strain by distortion of the naphthalene plane and the distortion results in splaying of the phenyl rings. The rings are pushed to opposite sides of the naphthalene plane and they also twist slightly so that they are not at 90° to the naphthalene plane. Selected measurements of compounds **12a** and **13a** are shown in Table 2. Comparison of the two data sets also reveals further interesting features. The first observation is that the amount of splaying of the 1,8-diaryl rings is decreased quite substantially when compared with the acenaphthene series.^{1b} It appears that substituents in the 2,7-positions on the naphthalene reduce the splaying effect by

**Fig. 7** Side view of **12a** (conformation 2).**Fig. 8** Side view of compound **13a**.

adding new steric repulsion to the aryl functions, resulting in forcing the 1,8-aryl functions closer together. The angle θ and the distance X measure the amount of splaying in the 2,7-naphthalene series (Table 2). The average angle for θ is 13.9° , while the average for the acenaphthene series is 19.2° .^{1b} The average for distance X in the two series is 2.95 versus 3.13 for the acenaphthene series.^{1b} Besides the additional repulsion of the isopropoxy functions in the 2,7-naphthalene series, it is also possible that absence of the acenaphthene benzylic bridge allows the two *peri*-aryl functions to move closer to each other. In the Cambridge Crystallographic Database, most structures with a naphthalene backbone have an X distance of 2.970–3.107 \AA , which is comparable to the X distances observed for **12a** and **13a**. Hence, it seems more probable that the reduction in the splaying is due more to having a naphthalene ring, rather than an acenaphthene backbone.

Table 3 ^1H Chemical shifts for 2,7-diisopropoxy-1,8-diphenylnaphthalenes **12a** and **13a**

Compound	H1/H1'	H2/H2'	H3/H3'	H4/H4'	H5/H5'	H6/H6'	Other signals
<i>anti</i> - 12a	7.77	7.17	4.96	6.41	6.16	6.61	1.02 -Me1/Me2 3.75 -OMe 2.01 -Me
<i>syn</i> - 12a	7.77	7.17	4.96	6.49	6.42	6.51	1.07 -Me1/Me2 3.75 -OMe 1.93 -Me
<i>anti</i> - 13a	7.78	7.19	4.15 (4.17) ^a	6.45	6.32	6.82	1.0 (0.95) -Me1/Me2 ^a 3.71 -OMe 1.30 - ^t Butyl
<i>syn</i> - 13a	7.76	7.18	4.14 (4.17) ^a	6.63	6.44	6.63	0.97 (0.93) -Me1/Me2 ^a 3.74 -OMe 1.27 - ^t Butyl

^a Diastereotopic, hence two peaks.

Comparison of the other measurements, *i.e.* τ_1 and ϕ , reveals that the isopropoxy unit does have some effect on the ground state geometry. Compounds **12a** and **13a** show some structural deviation in order to deal with different substituents. Firstly, **12a** has compensated for the increase in steric effects by increasing the movement of the phenyl rings to above and below the naphthalene plane (average angle ϕ is 9.38° for **12a** versus 7.17° for the corresponding acenaphthene system). Secondly, the rotation angle τ_1 is nearly 90° , which places the phenyl rings virtually perpendicular to the naphthalene plane. In contrast, compound **13a** has to compensate for its phenyl ring substituents by increasing the deformation of the phenyl rings on either side of the naphthalene plane; ϕ is almost identical when comparing **13a** (8.7°) and the corresponding acenaphthene system (9.2°). The change in the amount of splaying also results in a change in τ_1 , where the phenyl rings are at an angle of approximately 50° to the naphthalene plane (Table 2). However, it is unclear if these deviations are a direct result of having the isopropoxy substituents in the 2,7-positions. The X-ray structures only give a reflection of the ground state configuration and crystal packing forces could also have a large effect on the observed conformation, as well as the relative energy of the molecule.

Dynamic and structural NMR studies

Having isolated compounds **12a** and **13a**, we employed ^1H NMR spectroscopy to probe the rotational dynamics which operate in such systems. Thus, all dynamic ^1H NMR studies were measured at 600 MHz and longitudinal relaxation times were measured using the inversion-recovery technique. ROESY experiments were used to observe any NOE and exchange effects caused by rotation of the phenyl rings. The numbering scheme used for NMR assignment purposes for these molecules is shown in Fig. 9.

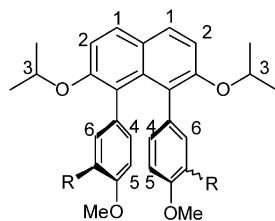


Fig. 9 Numbering scheme for **12a** and **13a**.

The ^1H NMR spectrum of compound **12a** showed that both the *syn*- and *anti*-atropisomers were present at ambient temperature, appearing as sharp well defined resonances (*vide supra*). The individual resonances were assigned as shown in Table 3, based upon integration, chemical shifts and couplings, in addition to NOEs measured from the ROESY experiments. However, the ROESY spectrum of **12a** indicated that slow

exchange was occurring. In molecule **12a** the barriers to interconversion are particularly large and therefore the rates of interconversion are very slow in comparison to the acenaphthene systems^{1b} (0.1 s^{-1} versus 2.4 s^{-1}). Due to the very slow exchange rates observed in **12a**, no line broadening effects or coalescence of the resonances are observed, making it impossible to use line shape analysis as a technique to calculate the rotation barriers. Instead, selective inversion experiments were used to obtain the rates of *syn-anti* interconversion over a range of temperatures (see Experimental section). The Eyring activation parameters were calculated from these exchange rates and the results are shown in Table 4, which gives rates of exchange and activation parameters.

The ^1H NMR spectrum of **13a** at 600 MHz showed that two atropisomers were present in solution with the predominant form being assigned to the *anti*-atropisomer. Observation of the *syn*-atropisomer was not apparent when the ^1H NMR spectrum was run at 300 MHz due to the high *anti* : *syn* ratio. The resonances shown in Table 4 were assigned based on integration, chemical shifts, couplings and NOEs. Again no line broadening effects or coalescence of the resonances were observed over a wide range of temperatures. Due to the slow exchange rates, selective inversion experiments were performed at various temperatures using the *tert*-butyl group and the calculation of exchange rates and activation parameters was carried out as previously described. However, due to the large ratio of *anti* : *syn* atropisomer these experiments proved to be difficult when inverting the *syn*-atropisomer *tert*-butyl group and only one inversion was successfully completed. The other rates were calculated from this rate, so the activation parameters for the *syn-anti* interconversion are assumed rather than calculated. The activation parameters are also shown in Table 4.

The effects of shielding on both compound **12a** and **13a** are identical. For the *anti-syn* interconversion of the substituents, *i.e.* for either the methyl or *tert*-butyl system, the *syn*-resonance is shifted upfield relative to the *anti*-resonance. The same effect is observed for H6/H6' (Table 3). However, the reverse is observed for H4/H4' and H5/H5'; the *anti-syn* interconversion results in the protons being shifted downfield. This observation is explained by the shielding effect of the aromatic system on the protons. When a proton is close to the centre of the aromatic system, it is shielded resulting in an upfield shift of the resonance; when compounds **12a** and **13a** are in the *syn*-geometry, the H4/H4' and H5/H5' protons are not affected by the aromatic system. However, rotation due to the *anti*-atropisomer places these two protons in close proximity to the aromatic system, which causes the resonances to shift upfield. In the case of the substituents on the *peri*-phenyl rings and the H6/H6' protons, the opposite effect is observed and when **12a** or **13a** is in the *syn*-geometry the phenyl substituents and the H6/H6' hydrogens are shielded by the aromatic system. This follows the same pattern as that which was observed for the acenaphthene series,^{1b} although the shielding effects are greater

Table 4 Activation parameters and rates of rotation for **12a** and **12b**

Compound	Activation enthalpy (ΔH) ^a /kcal mol ⁻¹	Activation entropy (ΔS) ^a /cal K ⁻¹ mol ⁻¹	Rotation barrier (ΔG) ^a /kcal mol ⁻¹	Rate of rotation/s ⁻¹ (K)
12a <i>anti-syn</i>	15.7	-8.07	18.2	0.111 (270 K)
<i>syn-anti</i>	15.6	-7.56	17.9	0.138 (270 K)
13a <i>anti-syn</i>	17.8	-0.42	17.9	0.085 (273 K)
<i>syn-anti</i>	17.8 ^a	5.17 ^a	16.3 ^a	—

^a Assumed values.**Table 5** Calculated biaryl rotational energy barriers for compounds **12a**, **13a** and **14** (enthalpy difference between the *anti*-conformer and the transition state of the aryl–aryl rotation)

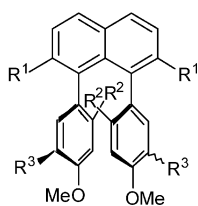
Compound	HF/3-21G*/kcal mol ⁻¹
14a	18.82
12a	20.89
13a	20.90
14b	37.69

in these molecules, with some aromatic resonances being shifted as far upfield as 6.16 ppm.

It is also worth noting that the energy barriers for **12a** and **13a** are essentially identical within experimental error; a phenomenon which was also previously observed in the acenaphthene series of compounds.^{1b} The explanation for the rotation barriers being similar is the fact that during rotation of a phenyl ring, the less hindered side of one ring is projected towards the flat face of the other phenyl ring and rotation can always occur away from the *meta*-substituent.

Molecular modelling

In order to probe the structural and dynamic features which operate in general systems **1**, we used *ab initio* molecular modelling methods to understand what processes control rotational dynamics. Hence, structures **12a**, **13a** and **14** were examined using quantum chemical calculations and the GAUSSIAN98 programme at the HF/STO-3G and HF/3-21G* levels of theory. Only the HF/3-21G* results were used for prediction of the heights of the energy barriers, as our earlier studies indicated better agreement between the results at this level and experiments.^{1b} Also in the present study the agreement between this method and the experimental measurements is rather good, indicating a reasonable compromise between accuracy and computational costs. The calculated energy barriers for structures **12a**, **13a** and **14** are displayed in Table 5. The corresponding structures (*anti*-conformations and transition states) are shown in Fig. 10.

**14**

- a**; R¹ = OMe, R² = H, R³ = ^tBu
b; R¹ = OMe, R² = Me, R³ = H

When we studied the rotation about the naphthyl–aryl torsion, we also investigated the influence of the conformations of the methoxy/isopropoxy groups adjacent to the rotating aromatic ring. To this end, the naphthyl–aryl torsion in molecule **14a** was changed in one-degree increments. The corresponding dihedral angle was fixed and the rest of the molecule fully relaxed with the adjacent methoxy group being located above and below the plane defined by the naphthyl ring, *i.e.* two geom-

etry optimisations were carried out for each of these points on the pathway of naphthyl–aryl rotation. These calculations were carried out for 25 points (or one-degree increments) before and after the transition state on this pathway and resulted in smooth and continuous energy profiles. It turned out that initially the energetically preferred orientation of the adjacent methoxy group was as shown for the *anti*-conformation of compound **14a** in Fig. 10 (herewith referred to as “below” the naphthyl plane when viewing the structure in Fig. 10 from the left-hand side). Fourteen points (or degrees) before the transition state for the naphthyl–aryl torsion is reached, the energetic preference of the adjacent methoxy group is shifted to “above” the naphthyl plane, as shown for the transition state of **14a** in Fig. 10. At this point of the pathway, calculation of the rotational barrier of the methoxy group to move from one conformation “below” to the other conformation “above” the naphthyl plane gave a value of 0.98 kcal mol⁻¹. The corresponding value for the isopropoxy group was very similar, and these calculations included location of the transition state for alkoxy rotation and characterization by frequency analysis. The associated activation energies are low compared to the energy that is still required to overcome the remaining energy barrier (*ca.* 8 kcal mol⁻¹) on the naphthyl–aryl torsional pathway. Transition state location for methoxy rotation in the local minimum of the *anti*-conformer of **14a** gave an activation barrier of 2.19 kcal mol⁻¹. Summarizing these data, the minimum energy pathway for *anti*–*syn* interconversion could be described as follows. Starting from the *anti*-conformer with the alkoxy group “below” the plane, *via* a transition state with respect to alkoxy rotation, an *anti*-conformer with the alkoxy group above the plane can be generated. This intermediate rotamer is slightly higher in energy, and the process that leads to it requires very little activation energy (*ca.* 2 kcal mol⁻¹). This implies that this intermediate rotamer is easily accessible throughout the process. The other transition state on the pathway corresponds to rotation about the naphthyl–aryl bond and the transition requires much more activation energy (*ca.* 20 kcal mol⁻¹). Therefore, the overall energy barrier is determined by the transition state on the naphthyl–aryl torsional pathway (Table 5). Taken together, one can consider the *anti*- to *syn*-interconversion in compounds **12a**, **13a** and **14** as the interplay of two linked rotors, *i.e.* rotation of both the alkoxy and the diaryl moieties, where the rotamers with respect to alkoxy rotation are energetically easily accessible.

The energies for biaryl rotation (see Table 5) indicate that the size of the substituents in the 2,7-positions (methoxy or isopropoxy in this study) has only a minor influence on the activation energy. Replacing the methoxy substituent with an isopropoxy group (**14a** versus **13a**) increases the activation enthalpy by 2.08 kcal mol⁻¹. The value of 20.90 kcal mol⁻¹ for compound **13a** is, however, too low to prevent the molecule from undergoing *anti*- to *syn*-interconversion at room temperature. Substituting a hydrogen atom in the *ortho*-position of the aryl moiety for a methyl group (*i.e.* **14a** versus **14b**) has a much more significant effect and increases the energy required for interconversion by almost 20 kcal mol⁻¹. Analysis of the geometry of the corresponding transition state (see Fig. 10) indicates that not only the naphthyl moiety deviates significantly from planarity (as in the other transition states), but the aryl ring itself is also severely distorted. The reason for this distortion is that the rotating ring

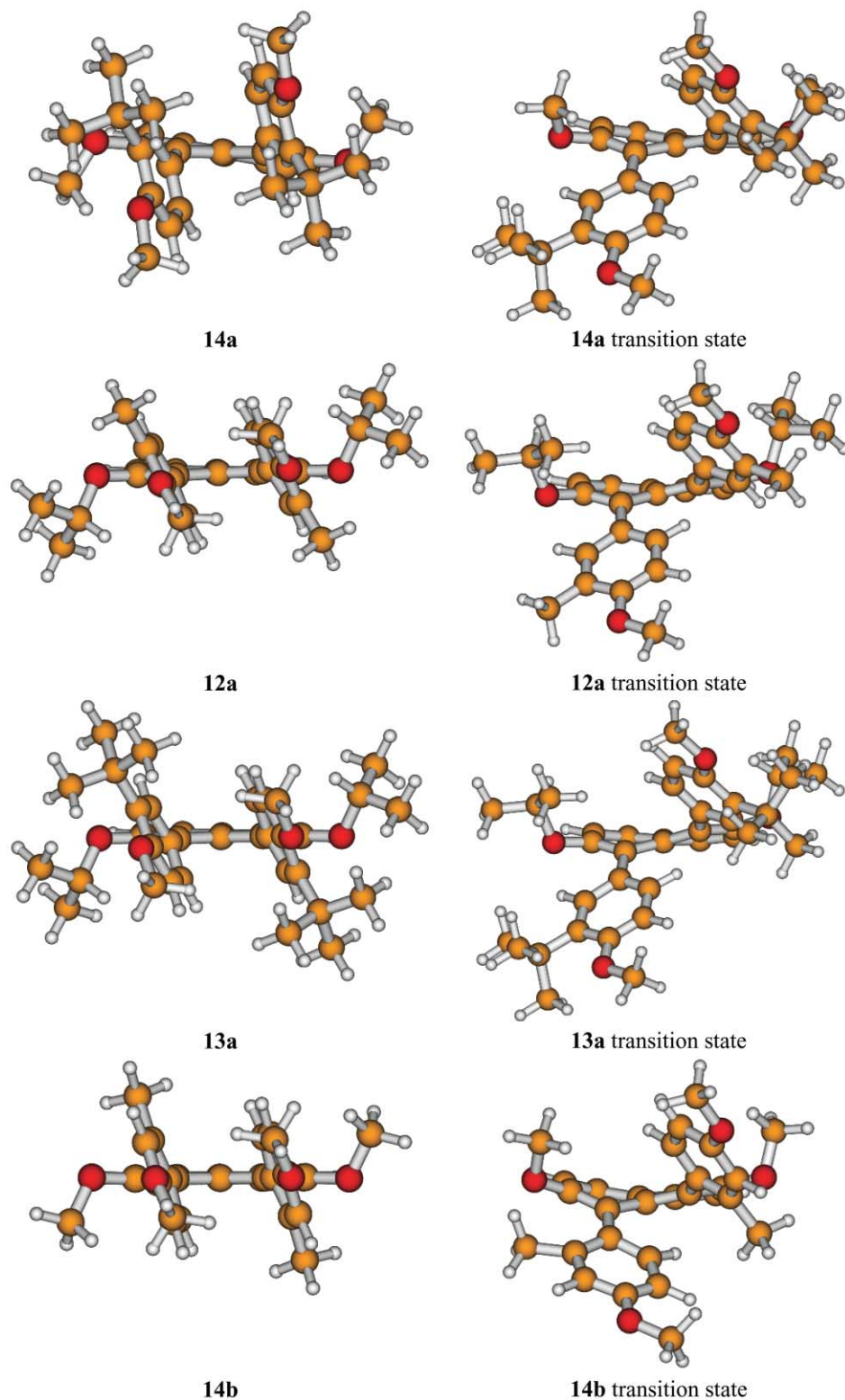


Fig. 10 Geometries of *anti* conformations and transition states of molecules **12a**, **13a**, and **14**.

becomes “wedged” between the adjacent aryl ring (distance *ortho*-H to *ortho*-C of adjacent ring: 2.68 Å) and the adjacent methoxy substituent (distance *ortho*-methyl C–oxygen of the methoxy group: 2.66 Å). As a consequence the activation energy rises to nearly 40 kcal mol⁻¹ for **14b**, which should be sufficient to prevent this molecule from interconverting at room temperature.

Summary and conclusion

The synthesis of highly hindered 1,8-diaryl-2,7-dialkoxy-naphthalene systems is far from straightforward, showing that

there is still a clear need to develop new coupling protocols which can be applied to such systems. However, it was possible to access compounds **12a** and **13a** and study both these compounds by both X-ray and NMR methods. Unfortunately, similar coupling reaction methods could not be applied to access a corresponding *ortho*-substituted 2,7-diisopropoxy-1,8-diphenylnaphthalene system. X-ray crystallographic studies on both **12a** and **13a** do however shed considerable light upon the extreme steric repulsions which operate in these systems, making preparation of the corresponding *ortho*-substituted-phenyl systems very challenging. The severe distortions shown by the X-ray structures are also mirrored by the dynamic NMR

spectroscopy, which shows extremely slow interconversion between *syn*- and *anti*-atropisomers, *i.e.* two orders of magnitude greater than we have observed before in systems which do not possess 2,7-dialkoxy functions on the naphthalene ring.^{1b} However, despite the success of the two dialkoxy functions in slowing rotation, these substituents are not sufficient to prevent the rotation process at room temperature; rotation barriers are in agreement with those of corresponding 2,7-unsubstituted systems^{1b} and those systems reported by Cozzi *et al.*,¹⁷ and reasonably well reproduced by *ab initio* calculations. The question therefore remains as to whether it is possible to ever stop the rotation process in systems of type **1**. *Ab initio* calculations perhaps provide the answer to this question; it is predicted that the addition of an *ortho*-methyl function onto the two 1,8-diphenyl rings in addition to 2,7-dialkoxy-naphthalene substituents (*i.e.* to provide structure **14b**), would result in a rotation barrier of the order of 40 kcal mol⁻¹, which should be sufficient to completely prevent all biaryl rotation at room temperature. In the light of this prediction, we are working towards the synthesis of such a system.

Experimental

General procedures and reagents

THF was freshly distilled under argon from benzophenone-sodium. Dichloromethane was freshly distilled under argon from calcium hydride. All other solvents were either purchased as anhydrous or used directly without further purification. 5,6-Dibromoacenaphthene,⁶ TBABr₃,⁷ and Pd(dba)₂/Pd₂(dba)₃·CHCl₃ were prepared⁸ as reported in the literature. Pd(PPh₃)₄ was prepared as reported in the literature⁹ and sealed under argon in glass ampoules for storage. All other reagents were purchased from Aldrich or Lancaster and were used without further purification unless stated otherwise.

Chromatography

Column chromatography was performed under medium pressure on silica gel (Merck, pore size 60 Å, 230–400 mesh). All anhydrous, low temperature reactions were carried out in glassware, which was dried prior to use in an oven at 140 °C and cooled under a stream of argon. All Suzuki coupling reactions were performed under strictly anaerobic conditions with all solvents being thoroughly degassed prior to use. All evaporations were carried out by partial evaporation on a Büchi rotary evaporator, followed by solvent drying *in vacuo* at approximately 0.5 mmHg. TLC was performed using Merck Kieselgel 60F₂₅₄ plastic backed plates or Fluka Kieselgel 60F₂₅₄ aluminium backed plates.

NMR spectroscopy

Room temperature ¹H NMR spectra were recorded at 300, 400 or 600 MHz on Bruker AC300, AC400 or AMX600 spectrometers respectively. ¹³C NMR spectra were recorded at 75.5 or 100 MHz on Bruker AC300 or AC400 spectrometers respectively. Both ¹H and ¹³C NMR spectra used residual incompletely deuterated solvent as the internal standard.

The samples of **12a** and **13a** used for ¹H NMR kinetic analysis were dissolved in CDCl₃, and all dynamic ¹H NMR measurements were made at 600 MHz. The assignments of the resonances were confirmed by 2-dimensional ROESY and TOCSY spectra, and ¹H-¹³C HSQC spectra. Exchange rates were measured by monitoring signal intensity changes following selective inversion of one of the two exchanging sites.¹⁰ For **12a**, in two separate experiments the *peri*-ring CH₃ signals of the *syn* and *anti* atropisomers were selectively inverted using the $\pi/2 - t_1 - \pi/2$ sequence of Robinson *et al.*,¹¹ whereas for **13a** the *anti ortho* aromatic proton signal due to H2 (6.82 δ) was select-

ively inverted using a soft 'sinc' pulse.¹² A separate experiment, inverting one of the *syn* aromatic signals, was not attempted because of their low intensity relative to the corresponding *anti* signal. Intensity changes of the *anti* signal during the return to equilibrium would therefore have been very small and derived exchange rates would include a large uncertainty. A relaxation delay of 12 s was used in these experiments, and during the return to equilibrium the intensities of the signals from the exchanging sites were monitored at 36 time intervals between 10 ms and 12 s. The analysis of the intensities, to give exchange rates, used the program *CIFIT*, derived¹³ from the earlier work of Muhandiram and McClung.¹⁴ Input to the *CIFIT* program includes approximate values for the spin-lattice relaxation times (T_1) of the exchanging sites, and these were obtained experimentally using the non-selective inversion-recovery technique. The dynamic NMR measurements were repeated at five temperatures in the range 270 to 330 K for **12a**, and six temperatures in the range 255 to 330 K for **13a**.

Molecular modelling

Quantum chemical calculations were carried out using the program Gaussian98.¹⁵ Initial geometry optimisations were performed at the HF/STO-3G level.¹⁶ The structures were then optimised further at the HF/3-21G* level.¹⁸ The geometries of stationary points were fully optimised without symmetry constraints. Harmonic vibrational frequencies were computed in order to characterize stationary points. Energy minima were confirmed as such by having no imaginary frequencies. Transition states were confirmed as first order saddle points by possessing exactly one imaginary frequency. Animation of the imaginary frequencies of the transition states indicated that the negative vibrational mode corresponded to the correct pathway of conformational transition. The energy barriers were calculated as the difference between minima and saddle point energies.

General characterisation

All melting points are uncorrected and were measured on a capillary melting point apparatus. Low resolution Fast Atom Bombardment (FAB) mass spectra were recorded on a Kratos MS50 mass spectrometer using an *m*-nitrobenzyl alcohol matrix. High-resolution electron impact (EI) mass spectra were recorded on a Kratos Concept IS spectrometer. Infrared spectra were recorded on a Perkin-Elmer 298 spectrometer as thin films on KBr plates or as KBr discs. UV-Vis spectra were recorded on a Perkin-Elmer 115 spectrometer. Microanalyses were performed using a Carlo-Erba 1106 elemental analyser. For compounds characterised without microanalysis, ¹H and ¹³C NMR were used to assess purity.

Preparation of 1,8-dibromonaphthalene-2,7-diol **4**

A mixture of 2,7-dihydroxynaphthalene **3** (1.0 g, 6.24 mmol), NBS (2.22 g, 12.4 mmol), CHCl₃ (100 cm³) and pyridine (0.148 g, 1.87 mmol) was stirred at room temperature for 4 hours. The resulting solution was washed with 10% HCl, water, dried (MgSO₄) and evaporated. The crude solid was recrystallised from ether-hexane to give compound **4** (1.2 g, 61%) as light brown crystals: mp 125 °C (Found: C, 38.0; H, 1.8; Br, 50.0. C₁₀H₆Br₂O₂ requires C, 37.8; H, 1.9; Br 50.2%); λ_{\max} (EtOH)/nm 312 (ϵ /dm³ mol⁻¹ cm⁻¹ 5855) and 241.5 (48993); ν_{\max} /cm⁻¹ (KBr disc) 3400 (OH), 1610 and 1510 (aromatics), 1350 (OH), 1180 (C–O), 840 (*para*-substituted aromatics) and 500 (C–Br); δ_{H} (300 MHz; DMSO) 7.09 and 7.71 (each 2 H, d, *J* 8.8, 2 × Ar-H), 10.58 (2 H, s, 2 × OH) (addition of D₂O causes signal at δ 10.58 to disappear); δ_{C} (75.5 MHz; DMSO) 101.6, 125.5, 131.7 and 155.3 (Ar-C), 115.3 and 131.7 (Ar-CH); *m/z* (FAB) 318/316 (M⁺, 30), 238 (M⁺ – Br, 8), 207 (M⁺ – O₂Br, 12%); *m/z* (EI) 315.8733 (M⁺, C₁₀H₆Br₂O₂ requires 315.8736).

Preparation of 2,7-diacetoxy-1,8-dibromonaphthalene 7

1,8-Dibromo-2,7-dihydroxynaphthalene **4** (2.0 g, 9.44 mmol), pyridine (3.73 g, 47.1 mmol), acetic anhydride (4.82 g, 47.1 mmol) and diethyl ether (100 cm³) were stirred at room temperature for 8 hours. The mixture was washed with dilute HCl (75 cm³), water (75 cm³), dried (MgSO₄) and evaporated. The resulting crude solid was recrystallised from chloroform–hexane to yield the product **7** (3.04 g, 82%) as pale brown crystals: mp 179–182 °C (Found: C, 42.0; H, 2.6; Br 39.5. C₁₄H₁₀O₄Br₂ requires C, 41.8; H, 2.5; Br, 39.7%); λ_{\max} (Et₂O)/nm 297.5 (ϵ /dm³ mol⁻¹ cm⁻¹ 7476) and 232.5 (69426); ν_{\max} /cm⁻¹ (KBr disc) 2940 (CH₃), 1765 [C(O)–O], 1610 and 1505 (aromatic), 1460 (CH₃), 1375 [O–C(O)–CH], 1200 (C–O) and 845 (C–Br); δ_{H} (300 MHz; CDCl₃) 2.44 (6 H, s, 2 × CH₃), 7.28 and 7.85 (each 2 H, d, *J* 8.8, 2 × Ar–H); δ_{C} (75.5 MHz; CDCl₃) 21.4 (CH₃), 114.15, 131.2, 133.3 and 149.7 (Ar–C), 122.8 and 130.4 (Ar–CH) and 169.0 (C=O); *m/z* (FAB) 402 (M⁺, 79), 361 (M⁺ – C₂H₂O, 100), 318 (M⁺ – C₄H₅O₂, 98), 43 (C₂H₆O₂⁺, 35%); *m/z* (EI) 399.8943 (M⁺, C₁₄H₁₀O₄Br₂ requires 399.8947).

Preparation of 2,7-diisopropoxynaphthalene 6 and 7-isopropoxy-2-naphthol 8

A solution of 2,7-dihydroxynaphthalene **3** (10 g, 62 mmol), potassium carbonate (25.88 g, 0.187 mol), tetrabutylammonium iodide (2.3 g, 6.24 mmol) and DMF (150 cm³) under argon was stirred for 1 hour. 2-Bromopropane (46 g, 0.374 mol) was added and the solution heated at 70 °C for 9 hours. After cooling to room temperature, DCM (150 cm³) was added followed by washing with 5% NaOH solution (150 cm³), water (5 × 200 cm³), drying (MgSO₄) and evaporation. The resulting crude product was purified by silica gel chromatography (petroleum ether : ethyl acetate, 50 : 1 as the eluent) to give two fractions. The first fraction was identified as 2,7-diisopropoxynaphthalene **6** (9.29 g, 61%) and obtained as a colourless solid: mp 49–51 °C (Found: C, 78.9; H, 8.3. C₁₆H₂₀O₂ requires C, 78.8; H, 8.3%); λ_{\max} (hexane)/nm 327 (ϵ /dm³ mol⁻¹ cm⁻¹ 4051), 319 (2145), 312.5 (2521), 299.0 (2299), 277.0 (3461), 268.5 (3276) and 235 (37179); ν_{\max} /cm⁻¹ (KBr disc) 3030 (Ar–H), 3000–2860 (CH₃, CH₂), 1620 and 1510 (aromatic), 1390 and 1370 (CH₃), 1210 and 1110 (Ar–O–C) and 820 (*para*-substituted aromatic); δ_{H} (300 MHz; CDCl₃) 1.41 and 1.43 (each 6 H, s, 2 × CH₃), 4.71 (2 H, sept, *J* 6.0, 2 × CH), 6.98 (2 H, dd, *J* 9.0 and 2.3, 2 × Ar–H), 7.05 (2 H, d, *J* 2.3, 2 × Ar–H) and 7.66 (2 H, d, *J* 9.0, 2 × Ar–H); δ_{C} (75.5 MHz; CDCl₃) 22.5 (CH₃), 70.2 [OCH(CH₃)₂], 108.2, 117.5 and 129.5 (Ar–CH), 124.5, 136.4 and 156.7 (Ar–C); *m/z* (FAB) 244 (M⁺, 100), 160 (M⁺ – C₆H₁₂, 83), 43 (C₃H₇⁺, 21%); *m/z* (EI) 244.1464 (M⁺, C₁₆H₂₀O₂ requires 244.1463). The second fraction was 7-isopropoxy-2-naphthol **8** (2.26 g, 18%) and obtained as a colourless solid: mp 96–98 °C; λ_{\max} (Et₂O)/nm 328 (ϵ /dm³ mol⁻¹ cm⁻¹ 3615), 320 (2153), 313.5 (2500), 282 (3369) and 234.5 (97564); ν_{\max} /cm⁻¹ (KBr disc) 3460 br (OH), 2990–2880 (CH₃, CH), 1610 and 1510 (aromatic), 1390 (CH₃), 1270 (OH), 1200 (C–O) and 840 (*para*-substituted aromatic); δ_{H} (300 MHz; CDCl₃) 1.40 and 1.42 (each 3 H, s, CH₃), 4.70 [1 H, sept, *J* 6.0, CH(CH₃)₂], 5.01 (1 H, br s, OH) (signal disappears on addition of D₂O), 6.91–6.98 (2 H, m, 2 × Ar–H), 7.00 (1 H, s, Ar–H), 7.04 (1 H, d, *J* 2.6, Ar–H), 7.67 (2 H, d, *J* 8.7, 2 × Ar–H); δ_{C} (75.5 MHz; CDCl₃) 22.4 (CH₃), 70.2 [O–CH(CH₃)₂], 107.6, 109.0, 115.5, 117.7, 129.7 and 129.9 (Ar–CH), 124.7, 136.4, 154.3 and 156.2 (Ar–C); *m/z* (FAB) 202 (M⁺, 95), 160 (M⁺ – C₃H₆, 100), 43 (C₃H₇⁺, 19%); *m/z* (EI) 202.0992 (M⁺, C₁₃H₁₄O₂ requires 202.0994).

Preparation of 1,8-dibromo-2,7-diisopropoxynaphthalene 5

A solution of NBS (4.96 g, 27.9 mmol) in CHCl₃ (68 cm³) under argon was treated with pyridine (2.21 g, 27.9 mmol). The mixture was heated at reflux for 1 hour (all NBS had dissolved and the solution turned from colourless to orange). A solution

of 2,7-diisopropoxynaphthalene **6** (1.70 g, 6.97 mmol) in chloroform (~5 cm³) was added dropwise, followed by heating at reflux for 9 hours. After cooling to room temperature and evaporation, the crude reaction mixture was purified by silica gel chromatography (petroleum ether : ethyl acetate, 50 : 1 as eluent) to provide a solid which was re-crystallised from DCM–petroleum ether to yield the product **5** (1.096 g, 40%) as a brown–orange crystalline solid: mp 113 °C (Found: C, 47.5; H, 4.6; Br 40.0. C₁₆H₁₈Br₂O₂ requires C, 47.8; H, 4.5; Br 39.8%); λ_{\max} (Et₂O)/nm 311 (ϵ /dm³ mol⁻¹ cm⁻¹ 6070) and 246.5 (66069); ν_{\max} /cm⁻¹ (KBr disc) 2980 and 2920 (CH₃), 1610 and 1510 (aromatic), 1380 and 1370 (CH₃), 1260 (Ar–C–O), 1105 (C–O–C), 830 (two adjacent aromatic H's) and 620 (C–Br); δ_{H} (300 MHz; CDCl₃) 1.43 and 1.45 [each 6 H, s, CH(CH₃)₂], 4.69 (2 H, sept, *J* 6.0, 2 × CH(CH₃)₂), 7.13 and 7.68 (each 2 H, d, *J* 9.0, 2 × Ar–H); δ_{C} (75.5 MHz; CDCl₃) 22.8 (CH₃), 74.0 [CH(CH₃)₂], 109.4, 128.3 and 155.8 (Ar–C), 116.1 and 129.9 (Ar–CH); *m/z* (FAB) 402 (M⁺, 100), 318 (M⁺ – C₆H₁₂, 95), 43 (C₃H₇⁺, 100%); *m/z* (EI) 399.9675 (M⁺, C₁₆H₁₈Br₂O₂⁺ requires 399.9675).

Cross coupling of 1,8-dibromo-2,7-diisopropoxynaphthalene 5 with 4-methoxy-3-methylphenylboronic acid 9

A mixture of 1,8-dibromo-2,7-diisopropoxynaphthalene **5** (0.6 g, 1.49 mmol), 4-methoxy-3-methylphenylboronic acid **9** (0.54 g, 3.27 mmol), barium hydroxide octahydrate (1.88 g, 5.96 mmol), DMA (15 cm³) and water (3 cm³) in a Rotaflo™ tube was degassed using a freeze–pump–thaw method (3 cycles). After the addition of Pd(PPh₃)₄ (0.17 g, 0.149 mmol) and repeated degassing (3 cycles), the mixture was heated under argon at 70–80 °C for 72 hours. After cooling to room temperature, the mixture was diluted with DCM (15 cm³), washed with 10% HCl (4 × 20 cm³), dried (MgSO₄) and evaporated. The crude product was purified using silica gel chromatography (petroleum ether : ethyl acetate, 75 : 1 as eluent) to give 3 fractions. The first fraction was 2,7-diisopropoxy-1-(4-methoxy-3-methylphenyl)naphthalene **12c** (0.056 g, 10%); δ_{H} (300 MHz; CDCl₃) 1.16 and 1.29 [each 6 H, d, *J* 6.0, CH(CH₃)₂], 2.29 (3 H, s, CH₃), 3.93 (3 H, s, OCH₃), 4.36 and 4.45 [each 1 H, sept, *J* 6.0, CH(CH₃)₂], 6.93 (1 H, d, *J* 7.2, Ar–H), 6.94 (1 H, s, Ar–H), 7.01 (1 H, dd, *J* 9.0 and 2.0, Ar–H), 7.17 (3 H, m, 3 × Ar–H) and 7.84 (2 H, d, *J* 7.8, 2 × Ar–H); δ_{C} (300 MHz; CDCl₃) 16.6, 22.1 and 22.3 [CH(CH₃)₂], 22.8 (CH₃), 55.7 (OCH₃), 69.9 and 73.0 [CH(CH₃)₂], 107.6, 109.8, 116.7, 117.4, 128.4, 129.7, 129.8 and 133.8 (Ar–CH), 125.4, 126.1, 127.2, 128.9, 135.7, 153.5, 156.2 and 156.9 (Ar–C); *m/z* (FAB) 364 (M⁺, 100), 280 (M⁺ – C₆H₁₂, 60) and 43 (C₃H₇⁺, 20%); *m/z* (EI) 364.2025 (M⁺, C₂₄H₂₈O₃ requires 364.2038). The second fraction was 1-bromo-2,7-diisopropoxy-8-(4-methoxy-3-methylphenyl)naphthalene **12b** (0.25 g, 38%); mp 135–137 °C; λ_{\max} (Et₂O)/nm 311 (ϵ /dm³ mol⁻¹ cm⁻¹ 6205), 247 (48085) and 202.5 (31763); ν_{\max} /cm⁻¹ (KBr disc) 3000–2840 (CH₃, CH), 1610, 1580 and 1500 (aromatic), 1390 and 1370 (CH₃), 1260 (Ar–O–C), 1110 (C–O), 1030 (Ar–O–C), 830 (*para* substituted aromatic) and 560 (C–Br); δ_{H} (300 MHz; CDCl₃) 1.11 and 1.13 (each 3 H, s, CH₃), 1.36 and 1.39 (each 3 H, d, *J* 2.0, CH₃), 2.25 (3 H, s, CH₃), 3.90 (3 H, s, OCH₃), 4.39 and 4.60 [each 1 H, sept, *J* 6.0, CH(CH₃)₂], 6.83 (1 H, d, *J* 8.7, Ar–H), 7.00 (1 H, d, *J* 3.0, Ar–H), 7.01 (1 H, s, Ar–H), 7.11 (1 H, d, *J* 8.7, Ar–H), 7.21 (1 H, d, *J* 8.7, Ar–H) and 7.73 (2 H, dd, *J* 8.7 and 3.0, 2 × Ar–H); δ_{C} (75.5 MHz; CDCl₃) 16.5 [CH(CH₃)₂], 22.7 (CH₃), 55.7 (OCH₃), 73.0 and 73.9 [CH(CH₃)₂], 109.1, 116.0, 116.8, 129.4, 129.5, 130.4 and 134.6 (Ar–CH), 110.3, 125.0, 127.7, 128.3, 133.3, 154.9, 155.8 and 157.0 (Ar–C); *m/z* (CI) 443 (M⁺, 100), 363 (M⁺ – Br, 95%); *m/z* (ES) 443.1220 (M + H, C₂₄H₂₇BrO₃ requires 443.1222). The third fraction was 2,7-diisopropoxy-1,8-bis(4-methoxy-3-methylphenyl)naphthalene **12a** (0.204 g, 28%); mp 121–125 °C (Found: C, 79.5; H, 7.7. C₃₂H₃₆O₂ requires C, 79.3; H, 7.5%); λ_{\max} (hexane)/nm 305 (ϵ /dm³ mol⁻¹ cm⁻¹ 8484), 248 (55484) and 201 (42272); ν_{\max} /cm⁻¹ (KBr disc) 2980–2840 (CH₃, CH), 1610

and 1500 (aromatic), 1450 (C–H), 1390 and 1370 (CH₃), 1250 (Ar–O–C), 1140 and 1110 (C–O), 1040 (Ar–O–C) and 800 (*para* substituted aromatic); δ_{H} (300 MHz; CDCl₃) 0.98–1.05 [12 H, m, 2 × CH(CH₃)₂], 1.95 (3 H, s, CH₃), 2.02 (3 H, s, CH₃), 3.77 (6 H, s, 2 × OCH₃), 4.21 [2 H, dsept, *J* 6.0 and 1.9, 2 × CH(CH₃)₂], 6.32 (1 H, d, *J* 8.3, Ar-*H*), 6.40–6.57 (4 H, m, 4 × Ar-*H*), 6.63 (1 H, dd, *J* 8.3 and 2.3, Ar-*H*), 7.19 (2 H, d, *J* 9.0, 2 × Ar-*H*), 7.78 (2 H, d, *J* 9.0, 2 × Ar-*H*); δ_{C} (75.5 MHz; CDCl₃) 16.2 and 16.3 (CH₃), 22.7 (CH₃), 55.5 (OCH₃), 73.3 and 73.4 (OCH), 108.0, 109.0, 117.2, 117.3, 129.3, 130.2, 130.3 and 134.4 (Ar-*CH*), 124.0, 124.3, 127.4, 129.4, 130.7, 130.9, 155.1, 155.2, 155.4 and 155.5 (Ar-*C*); *m/z* (FAB) 484 (M⁺, 100), 400 (M⁺ – C₆H₁₂, 25), 279 (C₁₈H₁₅O₂⁺, 11), 43 (C₃H₇⁺, 15%); *m/z* (EI) 484.2619 (M⁺, C₃₂H₃₆O₄ requires 484.2613).

Cross coupling of 1,8-dibromo-2,7-diisopropoxynaphthalene 5 with 3-*tert*-butyl-4-methoxyphenylboronic acid 10

A mixture of 1,8-dibromo-2,7-diisopropoxynaphthalene **5** (1.0 g, 2.49 mmol), 3-*tert*-butyl-4-methoxyphenylboronic acid **10** (1.08 g, 5.22 mmol), barium hydroxide octahydrate (3.14 g, 9.94 mmol), water (5 cm³) and DMA (25 cm³) in a Rotaflo™ tube was degassed using the freeze–pump–thaw method (cycles). Tetrakis(triphenylphosphine)palladium(0) (0.286 g, 0.249 mmol) was added, the mixture was degassed as before (3 cycles) and heated to 80 °C for 72 hours. After cooling to room temperature, it was diluted with DCM (30 cm³), washed with 10% HCl (5 × 30 cm³) and evaporated. The resulting solid was purified by silica gel chromatography (petroleum ether : ethyl acetate, 100 : 1 as the eluent) to give a first fraction which was a mixture of **13c** mono-substituted product and **13a** doubly coupled product. Further purification of this mixture was achieved employing preparative HPLC using a Dynamax 60A reverse phase C18 preparative column (internal diameter 41.5 mm) with methanol (100%) as the eluent with a flow rate of 10 ml min⁻¹. The first fraction was **13c**: δ_{H} (300 MHz; CDCl₃) 0.96 and 1.01 [each 6 H, d, *J* 6.0, CH(CH₃)₂], 1.30 [18 H, s, 2 × C(CH₃)₃], 3.72 (6 H, s, 2 × OCH₃), 4.16 [2 H, sept, *J* 6.0, 2 × CH(CH₃)₂], 6.33 (2 H, d, *J* 8.3, 2 × Ar-*H*), 6.45 (2 H, dd, *J* 8.3 and 1.9, 2 × Ar-*H*), 6.82 (2 H, d, *J* 1.9, 2 × Ar-*H*), 7.20 and 7.79 (each 2 H, d, *J* 8.7, 2 × Ar-*H*); δ_{C} (100 MHz; CDCl₃) 22.6 and 22.7 [CH(CH₃)₂], 30.1 [C(CH₃)₂], 34.8 [C(CH₃)₃], 54.8 (OCH₃), 73.2 [OCH(CH₃)₂], 110.3, 117.5, 129.1, 130.3 and 130.5 (Ar-*CH*), 127.5, 130.1, 130.6, 134.9, 155.1 and 155.9 (Ar-*C*); *m/z* (FAB) 568 (M⁺, 100%); *m/z* (EI) 568.3566 (M⁺, C₃₈H₄₈O₂ 568.3721). The second fraction obtained from column chromatography was 1-bromo-8-(3-*tert*-butyl-4-methoxyphenyl)-2,7-diisopropoxynaphthalene **13b** (0.32 g, 27%): mp 113 °C (Found: C, 67.0; H, 6.8; Br, 16.2. C₂₇H₃₃O₃Br requires C, 66.8; H, 6.85; Br 16.5%); λ_{max} (Et₂O)/nm 310 (ϵ /dm³ mol⁻¹ cm⁻¹ 7,719), 245 (59,351) and 210 (31,098); ν_{max} /cm⁻¹ (KBr disc) 3000–2820 (CH₃, CH), 1610 and 1500 (aromatic), 1390 and 1360 (CH₃), 1230 (Ar–O–C), 1110 (C–O), 850 and 820 (*para*-substituted aromatics) and 630 (C–Br); δ_{H} (300 MHz; CDCl₃) 1.10, 1.14, 1.37 and 1.38 [each 3 H, d, *J* 6.0, CH(CH₃)₂], 1.40 [9 H, s, C(CH₃)₃], 3.91 (3 H, s, OCH₃), 4.38 and 4.61 [each 1 H, sept, *J* 6.0, CH(CH₃)₂], 6.88 (1 H, d, *J* 8.3, Ar-*H*), 6.99 (1 H, dd, *J* 8.3 and 2.3, Ar-*H*), 7.12 (1 H, d, *J* 8.7, Ar-*H*), 7.17 (1 H, d, *J* 2.3, Ar-*H*), 7.23 (1 H, d, *J* 8.8, Ar-*H*), 7.74 and 7.75 (each 1 H, d, *J* 8.7, Ar-*H*); δ_{C} (75.5 MHz; CDCl₃) 22.7 and 22.8 [CH(CH₃)₂], 30.3 [C(CH₃)₃], 35.1 [C(CH₃)₂], 55.5 (OCH₃), 73.0 and 74.0 [CH(CH₃)₂], 110.5, 127.8, 129.0, 130.1, 133.3, 136.8, 154.9, 155.8 and 157.9 (Ar-*C*), 110.8, 116.2, 116.9, 129.4, 129.5, 130.4

and 130.9 (Ar-*CH*); *m/z* (CI) 487.4/485.4 (M + H, 100), 405.5 (M⁺ – Br, 50%); *m/z* (ES) 485.1689 (M + H, C₂₇H₃₃O₃Br requires 485.1691).

Acknowledgements

We thank the EPSRC for studentships (to MS, GR/97311210 and RN, GR/98700139) and Dr H. Toms (QMUL) for assistance and advice with the selective inversion experiments. We thank Professor A. D. Bain (McMaster University, Canada) for advice and for providing the *CIFIT* software, and the University of London Intercollegiate Research Service (ULIRS) for access to the AMX600 spectrometer. We also wish to acknowledge the use of the EPSRC's Chemical Database Service at Daresbury.¹⁹

References

- (a) M. Steele, M. Watkinson and A. Whiting, *Perkin Trans. 1*, 2000, 588; (b) W. Cross, G. E. Hawkes, R. T. Kroemer, K. R. Liedl, T. Loerting, R. Nasser, R. G. Pritchard, M. Steele, M. Watkinson and A. Whiting, *Perkin Trans. 2*, 2000, 459; (c) R. G. Pritchard, M. Steele, M. Watkinson and A. Whiting, *Tetrahedron Lett.*, 2000, **41**, 6915; (d) N. C. Edge, J. J. James, C. A. McAuliffe, B. Beagley, N. Jaiboon, M. Thorpe, M. Watkinson, A. Whiting and D. Wright, *Tetrahedron*, 1996, **52**, 10193; (e) M. Watkinson, A. Whiting and C. A. McAuliffe, *J. Chem. Soc., Chem. Commun.*, 1994, 2141.
- R. L. Clough and J. D. Roberts, *J. Am. Chem. Soc.*, 1976, **98**, 1018.
- H. O. House, J. T. Holt and D. VanDerveer, *J. Org. Chem.*, 1993, **58**, 7516.
- (a) R. D. Wilson, *Tetrahedron*, 1958, **3**, 236; (b) R. D. Wilson, *J. Chem. Soc.*, 1965, 3304; (c) F. Bell, J. A. Gibson and R. D. Wilson, *J. Chem. Soc.*, 1956, 2335.
- (a) T. Watanabe, N. Miyaura and A. Suzuki, *Synlett.*, 1992, 207; (b) M. G. Johnson and R. J. Foglesong, *Tetrahedron Lett.*, 1997, **38**, 7001; (c) J. C. Anderson, H. Namli and C. A. Roberts, *Tetrahedron*, 1997, **53**, 15123.
- N. Tanaka and T. Kasai, *Bull. Chem. Soc. Jpn.*, 1981, **54**, 3020.
- C. K. Mihir, K. T. Abu, P. K. Bhisma, D. Deepa and K. Wancydora, *Tetrahedron Lett.*, 1998, **39**, 8163.
- L. Hegedus, B. Lipshutz, H. Nozoki, M. Reetz, P. Rittmeyer, K. Smith, F. Totter and H. Yamamoto, *Organometallics in Synthesis: A Manual*, Wiley, Chichester, 1995.
- D. R. Coulson, *Inorg. Synth.*, 1972, **13**, 121.
- T. Beringhelli, G. D'Alfonso, H. Molinari, G. E. Hawkes and K. D. Sales, *J. Magn. Reson.*, 1988, **80**, 45.
- G. Robinson, P. W. Kuchel, B. E. Chapman, D. M. Doddrell and M. G. Irving, *J. Magn. Reson.*, 1985, **63**, 314.
- (a) M. S. Silver, M. I. Joseph and D. I. Hoult, *J. Magn. Reson.*, 1984, **59**, 347; (b) R. Freeman, *Chem. Rev.*, 1991, **91**, 1397.
- A. D. Bain and J. A. Cramer, *J. Magn. Reson., Ser. A*, 1996, **118**, 21.
- D. R. Muhandiram and R. E. D. McClung, *J. Magn. Reson.*, 1987, **71**, 187.
- K. Raghavachari, J. B. Foresman, J. Cioslowski, J. V. Ortiz, A. G. Baboul, B. B. Stefanov, G. Liu, A. Liashenko, P. Piskorz, I. Komaromi, R. Gomperts, R. L. Martin, D. J. Fox, T. Keith, M. A. Al-Laham, C. Y. Peng, A. Nanayakkara, C. Gonzalez, M. Challacombe, P. M. W. Gill, B. Johnson, W. Chen, M. W. Wong, J. L. Andres, C. Gonzalez, M. Head-Gordon, E. S. Replogle and J. A. Pople, Gaussian, Inc., Pittsburgh PA, 1998.
- J. B. Collins, P. V. R. Schleyer, J. S. Binkley and J. A. Pople, *J. Chem. Phys.*, 1976, **64**, 5142.
- F. Cozzi, M. Cinquini, R. Annuziata and J. S. Siegel, *J. Am. Chem. Soc.*, 1993, **115**, 5330.
- J. S. Binkley, J. A. Pople and W. J. Hehre, *J. Am. Chem. Soc.*, 1980, **102**, 939.
- (a) D. A. Fletcher, R. F. McMeeking and D. Parkin, *J. Chem. Inf. Comput. Sci.*, 1996, **36**, 746; (b) F. H. Allen and O. Kennard, *Chem. Des. Autom. News*, 1993, **8**, 1–31.